

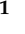


Article

Utilization of *Phyllanthus emblica* fruit stone as a Potential Biomaterial for Sustainable Remediation of Lead and Cadmium Ions from Aqueous Solutions

Sarita Kushwaha ¹, Suhas ^{1,*}, Monika Chaudhary ¹, Inderjeet Tyagi ², Rakesh Bhutiani ³ , Joanna Goscianska ⁴ , Jahangeer Ahmed ⁵ , Manila ¹ and Shubham Chaudhary ¹

- ¹ Department of Chemistry, Gurukula Kangri (Deemed to be University), Haridwar 249404, India; saritakushwaha31@gmail.com (S.K.); monikachoudry@gmail.com (M.C.); drmanilache@gmail.com (M.); shubhamchaudhary89@yahoo.com (S.C.)
- ² Centre for DNA Taxonomy, Molecular Systematics Division, Zoological Survey of India, Kolkata 700053, India; indertyagi011@gmail.com
- ³ Department of Zoology & Environmental Sciences, Gurukula Kangri (Deemed to be University), Haridwar 249404, India; rbhutiani@gmail.com
- ⁴ Department of Chemical Technology, Faculty of Chemistry, Adam Mickiewicz University in Poznań, Uniwersytetu Poznańskiego 8, 61-614 Poznań, Poland; asiagosc@amu.edu.pl
- ⁵ Department of Chemistry, College of Science, King Saud University, P.O. Box 2455, Riyadh 11451, Saudi Arabia; jahmed@ksu.edu.sa
- * Correspondence: suhas@gkv.ac.in; Tel.: +91-8791563015



Citation: Kushwaha, S.; Suhas; Chaudhary, M.; Tyagi, I.; Bhutiani, R.; Goscianska, J.; Ahmed, J.; Manila; Chaudhary, S. Utilization of *Phyllanthus emblica* fruit stone as a Potential Biomaterial for Sustainable Remediation of Lead and Cadmium Ions from Aqueous Solutions. *Molecules* **2022**, *27*, 3355. <https://doi.org/10.3390/molecules27103355>

Academic Editor: Eric Guibal

Received: 15 March 2022

Accepted: 12 May 2022

Published: 23 May 2022

Publisher's Note: MDPI stays neutral with regard to jurisdictional claims in published maps and institutional affiliations.



Copyright: © 2022 by the authors. Licensee MDPI, Basel, Switzerland. This article is an open access article distributed under the terms and conditions of the Creative Commons Attribution (CC BY) license (<https://creativecommons.org/licenses/by/4.0/>).

Abstract: In the present work, an effort has been made to utilize *Phyllanthus emblica* (PE) fruit stone as a potential biomaterial for the sustainable remediation of noxious heavy metals viz. Pb(II) and Cd(II) from the aqueous solution using adsorption methodology. Further, to elucidate the adsorption potential of *Phyllanthus emblica* fruit stone (PEFS), effective parameters, such as contact time, initial metal concentration, temperature, etc., were investigated and optimized using a simple batch adsorption method. It was observed that 80% removal for both the heavy metal ions was carried out within 60 min of contact time at an optimized pH 6. Moreover, the thermodynamic parameters results indicated that the adsorption process in the present study was endothermic, spontaneous, and feasible in nature. The positive value of entropy further reflects the high adsorbent–adsorbate interaction. Thus, based on the findings obtained, it can be concluded that the biosorbent may be considered a potential material for the remediation of these noxious impurities and can further be applied or extrapolated to other impurities.

Keywords: *Phyllanthus emblica* fruit stone; lead; cadmium; biosorption; pseudo-second order kinetic model; adsorption isotherm

1. Introduction

Water, being the most essential element and basic requirement of the living creatures on Earth, constitutes >70% of the entire earth's surface, out of which only 0.002% is considered appropriate for human consumption [1]. Due to rapid urbanization and industrialization, it is a very tough challenge for us to prevent this precious resource from getting polluted [2]. Pollutants containing different heavy metal ions from various sources, such as oil refining, tannery, paints, batteries, electrical, metal plating, pigments and chemical manufacturing were discharged into our water resources [3,4]. Other than the external heavy metals (HMs) polluting sources, they are present as natural constituents with varying concentrations in the Earth's crust [5]. These heavy metal ions get accumulated as a toxicant in the aquatic biota and possess a severe detrimental adverse impact on human and faunal health. The HMs are considered persistent environmental pollutants due to their availability for several years in the complex food web network [5]. Among these HMs, in the present

work, we consider Pb(II) and Cd(II) as model pollutants as they are broadly distributed across the environment and thereby develop chances for an average person to come into contact with them. Literary pieces of evidence supported the fact that chronic exposure of Pb(II) in humans causes reproductive and neurological disorders and also possesses certain genotoxic as well as carcinogenic effects on human health. On the other hand, chronic exposure of Cd(II) causes different malfunctions, such as lesions, pulmonary cancer, nephrological and osteological disorders, etc. [6–8].

Keeping in view the severe toxicity of these metal ions, the US Environmental Protection Agency (USEPA) prescribed 1.0 mg L^{-1} as the maximum permissible concentration of Pb in industrial wastewater and 0.015 mg L^{-1} in drinking water, while the Indian agency, the Central Pollution Control Board (CPCB) limits it to 0.1 mg L^{-1} as the maximum permissible concentration in the inland surface water. The Bureau of Indian Standards recommended 0.01 mg L^{-1} as the maximum admissible limit of Pb(II) concentration in drinking water. Moreover, the environmental and health agencies, such as USEPA, WHO and CPCB, prescribe 0.005 , 0.003 and 0.003 mg L^{-1} , respectively, as the maximum permissible limit of Cd(II) in the drinking water beyond this limit, with continuous exposure, may lead to several health hazards, as discussed in the preceding paragraphs.

Thus, based on the properties of HMs, such as their ubiquitous nature; long-term stability; high toxicity, even in trace concentrations; a tendency to bio-accumulate, etc., led to heavy metal pollution to become a relatively scorching issue that needs to be addressed with immediate effect regarding the advent of new technologies. To date, different techniques [9,10], such as reverse osmosis, coagulation/flocculation, ion exchange, precipitation, biosorption, etc., have been used for the removal of metals, and each has certain advantages as well as disadvantages. However, it is worthwhile to note that out of these, the biosorption process through accumulation—with the help of biological material—helps in the restoration or disposal of the pollutants in an acceptable range by removing them from water [11]. Further, the biosorption process has several advantages, such as being economical, sludge free, providing the restoration of sorbate, and being highly selective for pollutants and their removal efficiency [12,13].

A number of biomasses [8,14–23] have been used for the biosorption process viz., wheat straw, apple pomace, rice husk, jujube shell, orange peels, *Orbignya speciosa*, *Phyllanthus emblica* bark, *Phyllanthus emblica* leaf powder, etc. Owing to their low market value and abundance, the natural biomass material may act as a promising choice for biosorption. *Phyllanthus emblica* fruit stone (PEFS), an important lignocellulosic carbonaceous biomass, is available in significant amounts in India. The fruit of *Phyllanthus emblica* (PEF) has many medicinal values [24] and is utilized for a variety of long-established curing of diseases in India. Furthermore, PEF [25,26] is also used in making traditional edible foodstuffs, such as jams, jellies, tarts, chutneys, etc., and after removing the pulp from *emblica* fruit, the remaining fruit stone is more or less a waste. Due to the large use of PEF, a massive number of fruit stones are disposed of as waste per year, which are not perilous and may be utilized for other purposes. It is worth mentioning, however, that except few marginal applications, PEFS does not have any major utility in industry, hence, they can be used for the removal of harmful metals.

Hence, in the present work, we used a biosorbent PEFS and applied it for the sustainable remediation of noxious Pb(II) and Cd(II) from aqueous solutions. To be specific, the significant objectives of the current work are: (1) To utilize biomass PEFS as a biosorbent and to explore its potential in remediation of Pb(II) and Cd(II); (2) to elucidate the impact of effective parameters, such as contact time, initial metal ion concentration, pH and temperature on the remediation of noxious Pb(II) and Cd(II) from the aqueous solutions; (3) to explore the thermodynamics, kinetics and isotherm model that suited the adsorptive removal of selected model pollutants.

2. Results and Discussion

2.1. Effect of Contact Time

To determine the appropriate contact time for lead and cadmium metal ion removal by PEFS, the biosorption capacity for Pb(II) and Cd(II) was measured as a function of time at two different concentrations. The results acquired at 25 °C for Pb(II), are shown in Figure 1 and a similar trend is observed for Cd(II), therefore, not shown here. From Figure 1, it was observed that initially, the uptake of adsorbate species on the PEFS biosorbent was fast, which later becomes slow until equilibrium was achieved. The maximum amount (80%) of lead and cadmium metal ion was removed in less than 60 min and thereafter, equilibrium was achieved in 120 min. Thus, for all equilibrium adsorption studies, the contact time was kept at 180 min and after this, no appreciable increase in the metal amount adsorbed was observed. This might be accredited to the rapid utilization of the freely accessible adsorbing sites [27] on the biosorbent surface.

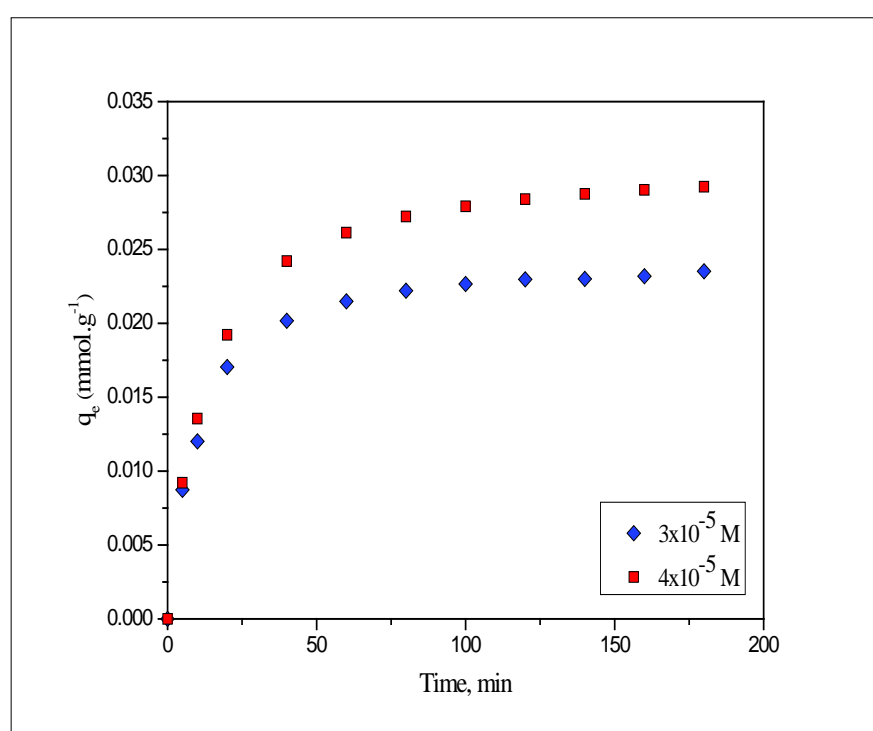


Figure 1. Effect of contact time and initial concentration on the biosorption of (a) Pb(II) onto PEFS at 25 °C.

2.2. Effect of Initial Metal Ion Concentration

The effect of variation in the initial concentration of Pb(II) and Cd(II) on the biosorption process of the PEFS was also elucidated. The amount of lead and cadmium metal ions adsorbed on the PEFS at two different concentrations, 3×10^{-5} and 4×10^{-5} M for Pb(II), and 2×10^{-5} and 3×10^{-5} M for Cd(II), was studied. The results obtained for Pb(II) are presented in Figure 1. Experimental observation from the results revealed that with the increase of the initial metal ion concentration, the amount of Pb(II) and Cd(II) adsorbed per unit mass of the PEFS increased; however, the percentage of the biosorption was found to decrease. This may be due to the fact that at low metal ion concentrations, all the metal ions present in the aqueous solution might interact with the binding sites present on the biosorbent, thus, the percentage of the biosorption was greater in contrast to the higher concentration [28].

2.3. Effect of pH

The pH level is one of the important key parameters that influence the sorption efficiency by affecting the solubility of the metal and the total charge of the biosorbent functional group [29]. In this study, the effect was investigated within the pH range (2–7) keeping other parameters constant (contact time: 180 min, adsorbent dose: 0.01 g/10 mL, temperature: 25 °C, metal ion concentration: 3×10^{-5} M). Experiments were not conducted at higher pH as lead as well as cadmium metal ions were hydrolyzed and precipitated in an alkaline medium instead of their adsorption [30]. The amount of the Pb(II) and Cd(II) removed at different pH is presented in Figure 2. At lower pH [31], removal of the lead and cadmium was inhibited due to the competition between the metal ions and hydrogen ions for adsorption sites present on the biosorbent surface, thus making it inaccessible for the metal binding [32]. Whereas, at higher pH, the lower amount of protons in the solution results in the reduced competition with the metal ions to be biosorbed onto the surface of PEFS. This fact is also supported by the point of zero charge ($\text{pH}_{\text{PzC}} = 3.4$) of PEFS. More cations, namely Pb(II) and Cd(II) are adsorbed onto the surface of PEFS at $\text{pH} > \text{pH}_{\text{PzC}}$, as the surface of the PEFS becomes negatively charged, thereby enabling for the biosorption of positively charged metal ions due to the electrostatic attraction and less competition with protons.

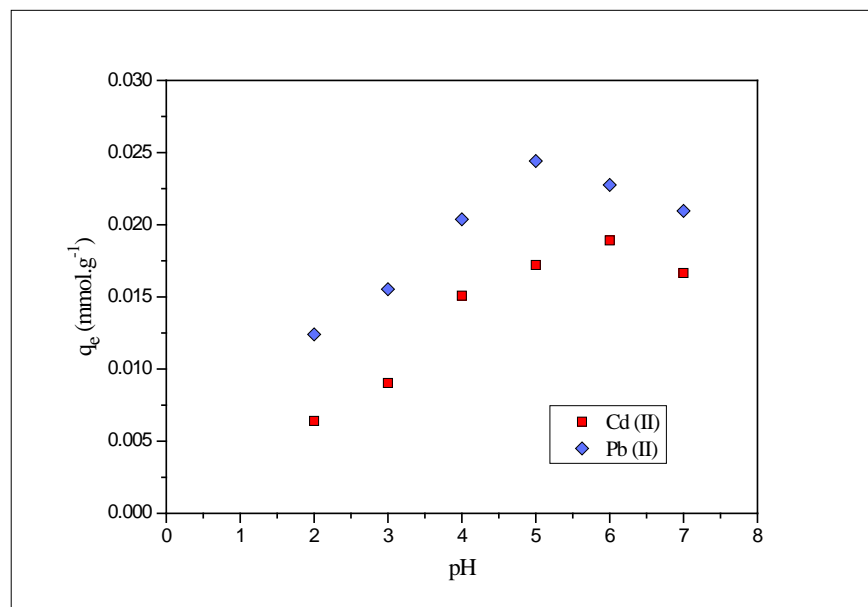


Figure 2. Effect of pH on the biosorption of Pb(II) and Cd(II) onto PEFS at 3×10^{-5} M.

The amount of lead metal ion adsorbed increased on increasing the pH from 2 to 5 and further removal decreased with an increase in the pH from 5 to 7. The maximum removal efficiency was obtained at pH 5; hence, all further experimental studies were carried out at pH 5. Similarly, for cadmium metal ions, the amount adsorbed increased from pH 2–6 and decreased further from 6–7, the maximum amount adsorbed at pH 6, hence, all the experiments were further carried out at pH 6.

2.4. Adsorption Isotherms

Adsorption isotherm defines the relation between the quantity of the adsorbate adsorbed by the biosorbent material and the concentration of the adsorbate remaining in the solution after the system attained the equilibrium at a constant temperature. In order to evaluate the effectiveness of the PEFS for the removal of the metal ion, the equilibrium sorption of the Pb(II) and Cd(II) was studied as a function of the concentration and the adsorption isotherm obtained is shown in Figure 3.

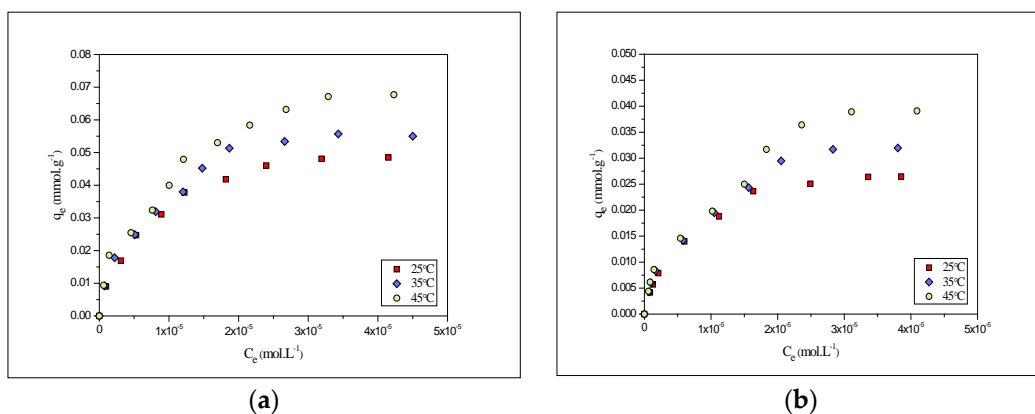


Figure 3. Adsorption isotherms of (a) Pb(II) and (b) Cd(II) onto PEFS at 25, 35 and 45 °C.

The experimental values obtained at 25, 35 and 45 °C were found to be 0.048, 0.055 and 0.068 mmol·g⁻¹ for Pb(II) and 0.026, 0.032 and 0.039 mmol·g⁻¹ for Cd(II), respectively. Comparative results clearly show that Pb(II) removal is more than compared to Cd(II).

Further, the adsorption isotherm models, such as Langmuir and Freundlich, were applied to optimize the sorption process isotherm data. The former isotherm model, i.e., the Langmuir isotherm model, was effectively used to reveal the monolayer sorption onto the fixed number of identical sites, and is represented using the equation mentioned below [33]:

$$\frac{1}{q_e} = \frac{1}{q_m} + \frac{1}{q_m b C_e} \quad (1)$$

where

The amount of model pollutant adsorbed at equilibrium is represented by q_e ;

The maximum monolayer adsorption capacity is measured by q_m ;

Langmuir equilibrium constant is represented by b ;

Equilibrium concentration is represented as C_e .

The Langmuir plots, i.e., $1/q_e$ and $1/C_e$ obtained for the biosorption of model pollutants Pb(II) and Cd(II) is shown in Figure 4.

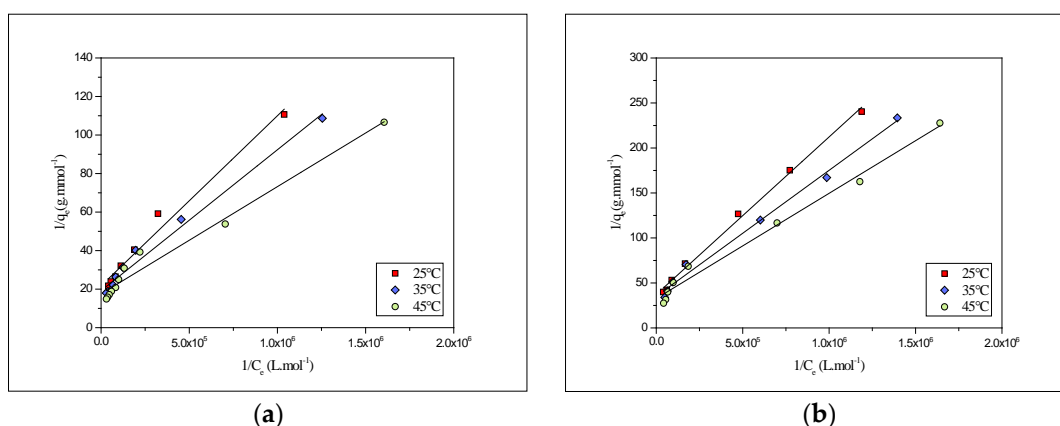


Figure 4. Langmuir adsorption isotherms of onto PEFS at 25, 35 and 45 °C for (a) Pb(II) and (b) Cd(II).

Further, the values of the maximum monolayer adsorption (q_m) and Langmuir constant (b) were measured from the intercept and slope of the plot and are compiled in Table 1.

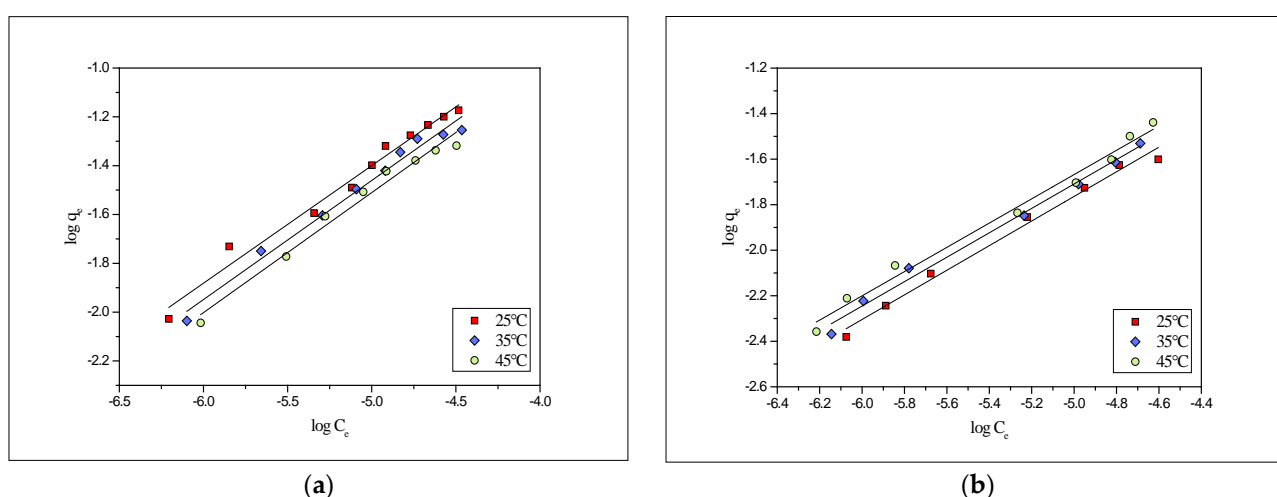
Table 1. Langmuir and Freundlich isotherm constants and correlation coefficients for biosorption Pb(II) and Cd(II) onto PEFS at different temperatures.

Metals	Temp (°C)	Langmuir			Freundlich		
		q_{\max} (mmol·g ⁻¹)	b (L·mol ⁻¹)	R ²	K_f (mmol·g ⁻¹)	n	R ²
Pb(II)	25	0.048	2.36×10^5	0.980	8.90	2.03	0.980
	35	0.052	2.62×10^5	0.984	9.54	2.05	0.984
	45	0.057	3.15×10^5	0.974	10.20	2.08	0.981
Cd(II)	25	0.027	2.13×10^5	0.996	8.71	1.85	0.990
	35	0.028	2.51×10^5	0.992	9.37	1.87	0.991
	45	0.031	2.80×10^5	0.987	9.92	1.88	0.988

On the other hand, the Freundlich adsorption isotherm model was used to reveal the multilayer adsorption and was based on the theory of the multilayer sorption process [34]. It was represented linearly using the equation mentioned below:

$$\log q_e = \log k_F + (1/n) \log C_e \quad (2)$$

where q_e is the amount of the metal adsorbed at the equilibrium concentration C_e , k_F (mmol·g⁻¹) (L·mol⁻¹)^{1/n} and n (unitless) represented constants linked with adsorption capacity and adsorption intensity, respectively. Freundlich plots between $\log C_e$ and $\log q_e$ for the adsorption of the Pb(II) and Cd(II) are given in Figure 5. Values obtained for all the isotherm constants and correlation coefficients are tabulated in Table 1. From the tabulated values (Table 1), it can be observed that both the Langmuir and Freundlich models follow well to the experimental data in both cases Pb(II), as well as Cd(II). The results of the adsorption process show that the adsorption of the lead is higher than the cadmium on the PEFS. This may be due to the fact that ionic radius plays an important role in the adsorption of metal on the biosorbent surface. Though the lead and cadmium have the same valency, the ionic radius of the lead was larger than the cadmium and, thus, owing to the smaller size and higher charge densities, the cadmium ion will attract more water molecules and form larger hydrated ion in comparison to lead. Therefore, the access of the cadmium to the biosorbent surface will be less [35].

**Figure 5.** Freundlich adsorption isotherms of onto PEFS at 25, 35 and 45°C for (a) Pb(II) and (b) Cd(II).

The shape of the isotherm may also indicate the favorability of the adsorption, which can be discussed by the parameter ' R_L ' [36]. It is termed an equilibrium parameter or separating factor and can be calculated using the equation mentioned below:

$$R_L = \frac{1}{1 + b C_0} \quad (3)$$

where the initial concentration is represented by C_0 and the Langmuir constant is represented by b . Further, values of R_L between 0 and 1 indicate a favorable adsorption isotherm [36].

2.5. Characterisation of PEFS and Mechanism

The work reported here is a further study of the biosorbent reported elsewhere [37], and some of the properties of the PEFS, as discussed elsewhere, are recapitulated in Table 2. Table 2 shows that the PEFS has a considerable carbon content (46.46%), whereas, among the inorganic contents (Table 2), calcium and potassium are found in large quantities as compared to the other inorganic elements. Pb and Cd were found to be nearly absent in the material. The stability of the PEFS in water was also tested, and it was found that the adsorbent does not dissolve in water, which makes it a perfect biosorbent. Furthermore, the functional groups observed on the surface of the PEFS were also determined with the help of Fourier transform infrared spectroscopy (FTIR) (Table 2). Besides this, the surface area of PEFS was found to be below, and the material was non-porous in nature, as discussed elsewhere [37]. Moreover, field emission scanning electron microscopy (FE-SEM) also favors this observation, as the surface of PEFS is compact in nature and non-porous.

Table 2. Characteristics properties of PEFS *.

Elemental Analysis of PEFS							
C%	N%	S%	H%				
46.5	0.07	0.14	6.2				
Inorganic Amount in 1 kg							
K (mg)	Na (mg)	Mg (mg)	Ca (mg)	Fe (mg)	P (mg)	Cu (mg)	Mn (mg)
432.2	253	101.3	860.14	26.7	267.99	5.4	0.81
FTIR Analysis of PEFS							
O-H stretching	C-H stretching	C=O stretching (carboxyl, aldehyde, ketone and ester)	carboxylate anion stretching	stretching due to Methoxy group	stretching due to ether and epoxide	C-O stretching of alcohol	-OH bending
3448	3000–2800 cm^{-1}	1740–1700 cm^{-1}	1637 cm^{-1}	1453 and 1423 cm^{-1}	1254 cm^{-1}	1044 cm^{-1}	615 cm^{-1}
XRD-analysis of PEFS							
2 θ = 16° and 22° Corresponding to cellulose							
N ₂ adsorption isotherms							
Low surface area and non-porous							
SEM analysis							
Compact surface structure							

* [37].

The biosorption behavior of metal ions on the PEFS is a plausible mechanism with physical adsorption, surface complexation, electrostatic attraction and ion exchange as conventional pathways in explaining the removal of Pb(II) and Cd(II) by PEFS [38,39]. The FTIR analysis (Table 2) of the PEFS shows that the main functional groups are -C-H, -OH, C=O, C-O, methoxy and carboxylate anion. Out of these, the carboxyl and hydroxyl group plays an important role in the removal of metal ions on the PEFS mechanism. Owing to the presence of these groups on the surface, PEFS attracts positively charged metal ions via electrostatic interactions and ion exchange methods. Finally, after these interactions, with the entrapping of metal ions in the PEFS surface, the complexation occurs, which is hypothesized via -COO and -OH interactions with Pb(II) and Cd(II) [38–41].

These functional groups, mainly the carboxyl and hydroxyl groups, get deprotonated at $\text{pH} > \text{pHpzc}$ and the metal ions (Pb^{2+} and Cd^{2+}) form complexes with the anionic form of these groups, resulting in the enhanced biosorption of the PEFS surface [32,42]. Therefore, it can be demonstrated that biosorption may occur through metal complexation [43,44] with the functional groups, such as hydroxyl and carboxyl present on the PEFS surface [32].

2.6. Effect of Temperature and Thermodynamic Parameters

To elucidate the effect of temperature, three different temperatures i.e., 25, 35 and 45 °C, were selected, and the findings obtained are shown in Figure 3. Results obtained indicated the fact that with the increase in temperature, the biosorption also increases. Thus, the process may be endothermic in nature. Further, the thermodynamic parameters, such as ΔG° (kJ mol^{-1}), ΔH° (kJ mol^{-1}) and ΔS° ($\text{J mol}^{-1} \text{K}^{-1}$) were also measured using the below-mentioned equations:

$$\Delta G^\circ = -RT \ln(b) \quad (4)$$

$$\ln b = -\frac{\Delta H^\circ}{RT} + \frac{\Delta S^\circ}{R} \quad (5)$$

where Universal gas constant ($8.314 \text{ J mol}^{-1} \text{K}^{-1}$) is denoted by R; the Temperature in Kelvin (K) is denoted by T and Langmuir's constant is denoted by b. Furthermore, the slope and intercept of the van't Hoff plot ($\ln b$ vs. $\frac{1}{T}$), as shown in Figure 6, was used to calculate the values of ΔH° and ΔS° , respectively. The results obtained for the thermodynamic parameters are compiled in Table 3.

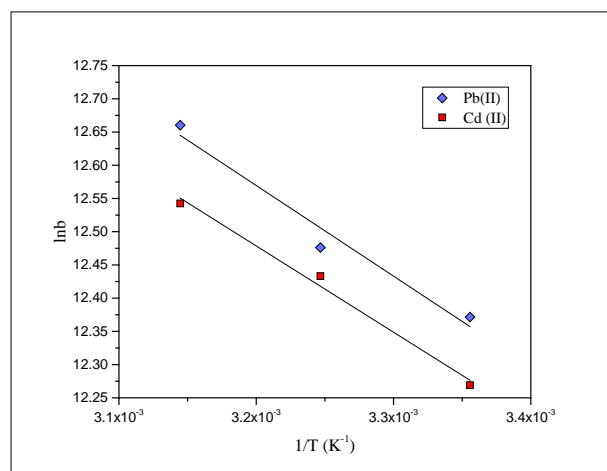


Figure 6. The van't Hoff plots for the biosorption of Pb(II) and Cd(II) onto PEFS.

Table 3. Thermodynamic parameters for biosorption of Pb(II) and Cd(II) onto PEFS.

Metals	Temperature (°C)	$-\Delta G^\circ$ ($\text{kJ}\cdot\text{mol}^{-1}$)	ΔS° ($\text{J}\cdot\text{mol}^{-1}\cdot\text{K}^{-1}$)	ΔH° ($\text{kJ}\cdot\text{mol}^{-1}$)
Pb(II)	25	30.7		
	35	30.9	141	11.3
	45	31.4		
Cd(II)	25	30.4		
	35	30.8	138	10.8
	45	31.1		

The positive value of ΔH° further confirmed that the adsorption process was endothermic in nature. Using the Langmuir constant, Gibbs free energy change, calculated at

different temperatures, was in the range of -30.7 to -31.4 and -30.4 to -31.1 kJ mol^{-1} for Pb(II) and Cd(II), respectively. However, these values are higher in the case of Pb(II) as compared to Cd(II). Thus, it can be concluded that the adsorption process at different temperatures was spontaneous in nature and thermodynamically feasible. Moreover, the positive values of ΔS° obtained from the van't Hoff plot for Pb(II) and Cd(II) indicate the affinity of the PEFS for the metals [45]. Hence, on the basis of thermodynamic studies, it can be concluded that the feasibility and spontaneity of the removal of Pb(II) are slightly more than Cd(II) on PEFS.

2.7. Biosorption Kinetics

The kinetic test for the biosorption of Pb(II) and Cd(II) at PEFS was carried out at different time intervals. The mechanism of the biosorption process was determined using different models [46–48] since different system conforms to different models. The kinetic model, such as pseudo-first order and pseudo-second order, were used to decipher the fitting to kinetic data. The Lagergren pseudo-first order kinetic equation [46], as mentioned below, was widely used:

$$\log (q_e - q_t) = \log q_e - \frac{k_1}{2.303} t \quad (6)$$

where q_e and q_t are the amounts adsorbed at equilibrium and time t , respectively, and k_1 is the pseudo-first order rate constant. A plot was made between $\log (q_e - q_t)$ vs. time t for Pb(II) and Cd(II) and is shown in Figure 7. The kinetic parameters were obtained using this and are presented in Table 4.

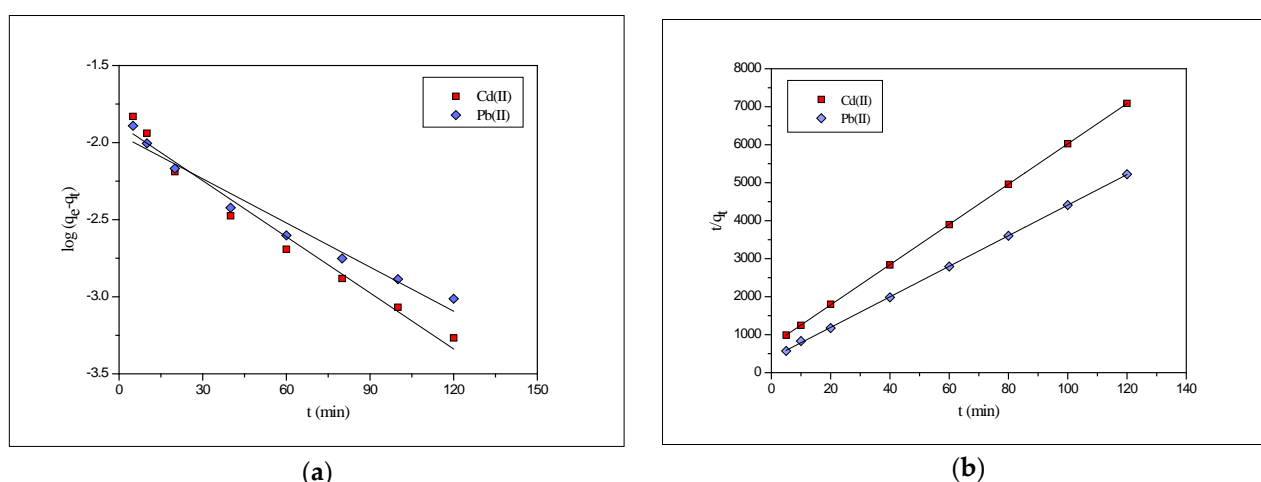


Figure 7. (a) Pseudo-first order; (b) pseudo-second order kinetic for the biosorption of Pb(II) and Cd(II) onto PEFS at 3×10^{-5} M.

Table 4. Kinetic parameters for the biosorption of Pb(II) and Cd(II) onto PEFS.

Metal	C_0 ($\text{mol} \cdot \text{L}^{-1}$)	q_e (exp) ($\text{mmol} \cdot \text{g}^{-1}$)	Pseudo-First Order			Pseudo-Second Order		
			q_e ($\text{mmol} \cdot \text{g}^{-1}$)	K_1 (min^{-1})	R^2	q_e ($\text{mmol} \cdot \text{g}^{-1}$)	K_2 ($\text{g} \cdot \text{mmol}^{-1} \cdot \text{min}^{-1}$)	R^2
Pb(II)	3×10^{-5}	0.024	0.013	0.019	0.743	0.025	4.19	0.998
Cd(II)	3×10^{-5}	0.018	0.011	0.022	0.969	0.019	3.88	0.999

Ho's second order equation [49] also known as the pseudo-second order kinetic model, was also used for the study and expressed as:

$$\frac{t}{q_t} = \frac{1}{K_2 q_e^2} + \frac{t}{q_e} \quad (7)$$

where the amount adsorbed at time t and equilibrium was denoted by q_t and q_e , respectively, and k_2 is the pseudo-second order rate constant. A plot made between t/q_t vs. t was presented in Figure 7 and the value of k_2 and q_e are determined from it. The results obtained were compiled in Table 4. Furthermore, it was observed that the value of the correlation coefficient (R^2) in the case of the pseudo-second order kinetic model was higher than that of the pseudo-first order kinetic model, and the experimental value of the amount adsorbed at the equilibrium (q_e) was in agreement with that of the calculated one obtained from the pseudo-second order model.

Moreover, the experimental amount adsorbed value ($q_{e(\text{exp})}$) was close to the calculated values ($q_{e(\text{cal})}$) of the pseudo-second order model, which confirms the fact that kinetic data in the present study fits well with the pseudo-second order kinetic model.

3. Materials and Methods

3.1. Chemicals

The chemicals used in the present work were of analytical grade. $\text{Pb}(\text{NO}_3)_2$ and $\text{Cd}(\text{NO}_3)_2 \cdot 4\text{H}_2\text{O}$ were purchased from Merck Specialties Private Limited, Mumbai, India and HiMedia Mumbai, India, respectively. Further, double-distilled water was used to prepare the experimental solutions and dilutions.

3.2. Preparation of PEFS

The PEFS was purchased from a local vendor. Further, the procured PEFS was subjected to multiple washing steps to remove the dust particles using distilled water and then oven-dried for 24 h at 100 °C. The dried PEFS materials were crushed into fine particles using a grinder and sieved to obtain a uniform particle size biomaterial. The obtained homogenous-sized biomaterial was stored in an airtight container until further application.

3.3. Preparation of the Solutions

A stock solution of the Pb(II) and Cd(II), with a concentration of 1×10^{-3} M, was prepared by dissolving the desired amount of $\text{Pb}(\text{NO}_3)_2$ and $\text{Cd}(\text{NO}_3)_2 \cdot 4\text{H}_2\text{O}$, respectively, in double-distilled water. A series of experimental solutions were prepared by the dilution of the stock solutions.

3.4. Adsorption Studies

Batch biosorption methodology was used to elucidate the effect of contact time, initial metal ion concentration and solution pH on Pb(II) and Cd(II) biosorption at PEFS. For this, in the stoppered glass tubes, a weighed amount (0.01 g) of the PEFS was added to 10 mL of the Pb(II) and Cd(II) solution of varying concentrations. All the solutions were kept under the desired temperature and agitated until the achievement of equilibrium using a temperature-controlled shaker bath. Further, the atomic absorption spectrophotometer (ECIL, AAS-4129, Hyderabad, India) was used to measure the concentration of model pollutants, i.e., Pb(II) and Cd(II) metal ions.

The amount of metal adsorbed onto the PEFS was measured as the difference between the metal adsorbed on the PEFS and the metal ions present in the solution after adsorption using the below-mentioned equation:

$$q_e = \frac{(C_0 - C_e)V}{W} \quad (8)$$

where

q_e is the metal uptake ($\text{mol} \cdot \text{g}^{-1}$);

C_0 and C_e are the initial and equilibrium concentrations ($\text{mol} \cdot \text{L}^{-1}$) in the solution, respectively,

V is the solution volume (L);

W is the mass (g) of the biosorbent used.

3.5. Characterisation of PEFS

The PEFS was characterized -in our previous work [37]. The inorganic elements in PEFS were investigated with the help of the inductively coupled plasma optical emission spectrometer (Perkin Elmer, model Optima 7000 DV, Waltham, MA, USA). An elemental analyser (Vario, Micro CHNS Analyser, Hesse, Germany) was used to study the weight percentages of carbon, hydrogen, nitrogen and sulfur in PEFS. The surface groups on PEFS were predicted with the help of Fourier transform infrared spectroscopy (FT-IR) by using the Perkin Elmer model Paragon 1000 PC spectrophotometer, Waltham, MA, USA. X-ray diffraction (XRD) patterns for PEFS were studied with an X-ray diffractometer Rigaku Smart Lab diffractometer, Tokyo, Japan. The surface morphology of PEFS was determined by field emission scanning electron microscopy (FE-SEM, Tescan Mira 3, Brno, Czech Republic).

4. Conclusions

The potential of PEFS has been tested for the sustainable remediation of noxious carcinogenic metal ions Pb(II) and Cd(II). Based on the results obtained, the following conclusions have been drawn:

1. The adsorption of Pb(II) and Cd(II) onto PEFS depends on the contact time, initial metal ion concentration, solution pH and temperature. The maximum amount (80%) of Pb(II) and Cd(II) ion was removed in less than 60 min and thereafter, equilibrium was achieved in 120 min.
2. The experimental sorption capacity for Pb(II) at pH 5 and Cd(II) at pH 6 with contact time 180 min and a biosorbent amount of 0.01 g was found to be 0.048 and 0.026 mmol·g⁻¹, respectively, at 25 °C.
3. Comparative results revealed that the removal of Pb(II) is more than that of Cd(II). The biosorption behavior of metal ions on the PEFS is a plausible mechanism with physical adsorption, surface complexation, electrostatic attraction and ion exchange as conventional pathways for explaining the removal of Pb(II) and Cd(II) by PEFS.
4. Kinetic data fits well with the pseudo-second order model, while the isotherm data fits well with both adsorption models, i.e., Langmuir and Freundlich.
5. The thermodynamic parameter shows that the biosorption process is spontaneous and favorable.
6. Keeping in view the results of the removal of Pb(II) and Cd(II), the biosorbent may be tried for wastewater/seawater containing these types of metal ions.

Author Contributions: Methodology, S.K. and S.; validation, S.K., J.G., J.A., S.C. and S.; formal analysis, S.K., M.C. and S.; investigation, S.K., M.C. and S.; resources, S.K. and S.; writing—original draft, S.K. and S.; writing—review and editing, M.C., R.B., J.G., J.A., S.C., I.T., S. and M.; visualization, S.K., J.G., J.A., S.C., M., R.B., I.T., M.C. and S.; supervision, S. All authors commented on previous versions of the manuscript. All authors have read and agreed to the published version of the manuscript.

Funding: The authors are thankful to DST, New Delhi, India, for their financial support under the Water Technology Initiative (Project No.: DST/TMD/EWO/WTI/2K19/EWFH/2019/90) and Researchers Supporting Project, number (RSP-2021/391) at King Saud University.

Institutional Review Board Statement: Not applicable.

Informed Consent Statement: Not applicable.

Data Availability Statement: Not applicable.

Acknowledgments: The authors are thankful to DST, New Delhi, India, for their financial support. One of the authors (Jahangeer Ahmed) would like to extend his sincere appreciation to the Researchers Supporting Project, number (RSP-2021/391), at King Saud University, Riyadh, Saudi Arabia for funding this research.

Conflicts of Interest: The authors declare no conflict of interest.

Sample Availability: Not applicable.

References

1. Alrumman, S.A.; El-kott, A.F.; Kehsk, M. Water pollution: Source and treatment. *Am. J. Environ. Eng.* **2016**, *6*, 88–98.
2. Gleeson, T.; Wada, Y.; Bierkens, M.F.P.; van Beek, L.P.H. Water balance of global aquifers revealed by groundwater footprint. *Nature* **2012**, *488*, 197–200. [[CrossRef](#)]
3. Ngah, W.S.W.; Hanafiah, M.A.K.M. Biosorption of copper ions from dilute aqueous solutions on base treated rubber (*Hevea brasiliensis*) leaves powder: Kinetics, isotherm, and biosorption mechanisms. *J. Environ. Sci.* **2008**, *20*, 1168–1176. [[CrossRef](#)]
4. Gupta, V.K.; Suhas; Nayak, A.; Agarwal, S.; Chaudhary, M.; Tyagi, I. Removal of Ni (II) ions from water using scrap tire. *J. Mol. Liq.* **2014**, *190*, 215–222. [[CrossRef](#)]
5. Song, H.-L.; Liang, L.; Yang, K.-Y. Removal of several metal ions from aqueous solution using powdered stem of *Arundo donax* L. as a new biosorbent. *Chem. Eng. Res. Des.* **2014**, *92*, 1915–1922. [[CrossRef](#)]
6. Wang, N.; Qiu, Y.; Hu, K.; Huang, C.; Xiang, J.; Li, H.; Tang, J.; Wang, J.; Xiao, T. One-step synthesis of cake-like biosorbents from plant biomass for the effective removal and recovery heavy metals: Effect of plant species and roles of xanthation. *Chemosphere* **2021**, *266*, 129129. [[CrossRef](#)]
7. Dahaghin, Z.; Mousavi, H.Z.; Sajjadi, S.M. Trace amounts of Cd(II), Cu(II) and Pb(II) ions monitoring using Fe₃O₄@graphene oxide nanocomposite modified via 2-mercaptobenzothiazole as a novel and efficient nanosorbent. *J. Mol. Liq.* **2017**, *231*, 386–395. [[CrossRef](#)]
8. Gupta, V.K.; Suhas. Application of low-cost adsorbents for dye removal—A review. *J. Environ. Manag.* **2009**, *90*, 2313–2342. [[CrossRef](#)]
9. Fu, F.; Wang, Q. Removal of heavy metal ions from wastewaters: A review. *J. Environ. Manag.* **2011**, *92*, 407–418. [[CrossRef](#)]
10. Mohapatra, R.K.; Parhi, P.K.; Pandey, S.; Bindhani, B.K.; Thatoi, H.; Panda, C.R. Active and passive biosorption of Pb(II) using live and dead biomass of marine bacterium *Bacillus xiamenensis* PbRPSD202: Kinetics and isotherm studies. *J. Environ. Manag.* **2019**, *247*, 121–134. [[CrossRef](#)]
11. Aksu, Z.; Dönmez, G. A comparative study on the biosorption characteristics of some yeasts for Remazol Blue reactive dye. *Chemosphere* **2003**, *50*, 1075–1083. [[CrossRef](#)]
12. Aksu, Z.; Karabayır, G. Comparison of biosorption properties of different kinds of fungi for the removal of Gryfalan Black RL metal-complex dye. *Bioresour. Technol.* **2008**, *99*, 7730–7741. [[CrossRef](#)]
13. Tounsadi, H.; Khalidi, A.; Abdennouri, M.; Barka, N. Biosorption potential of *Diplotaxis harra* and *Glebionis coronaria* L. biomasses for the removal of Cd(II) and Co(II) from aqueous solutions. *J. Environ. Chem. Eng.* **2015**, *3*, 822–830. [[CrossRef](#)]
14. Safa, Y.; Bhatti, H.N. Biosorption of Direct Red-31 and Direct Orange-26 dyes by rice husk: Application of factorial design analysis. *Chem. Eng. Res. Des.* **2011**, *89*, 2566–2574. [[CrossRef](#)]
15. Gorgievski, M.; Božić, D.; Stanković, V.; Štrbac, N.; Šerbula, S. Kinetics, equilibrium and mechanism of Cu²⁺, Ni²⁺ and Zn²⁺ ions biosorption using wheat straw. *Ecol. Eng.* **2013**, *58*, 113–122. [[CrossRef](#)]
16. Chand, P.; Bafana, A.; Pakade, Y.B. Xanthate modified apple pomace as an adsorbent for removal of Cd (II), Ni (II) and Pb (II), and its application to real industrial wastewater. *Int. Biodeterior. Biodegrad.* **2015**, *97*, 60–66. [[CrossRef](#)]
17. do Nascimento, J.M.; de Oliveira, J.D.; Leite, S.G.F. Chemical characterization of biomass flour of the babassu coconut mesocarp (*Orbignya speciosa*) during biosorption process of copper ions. *Environ. Technol. Innov.* **2019**, *16*, 100440. [[CrossRef](#)]
18. Znad, H.; Awual, M.R.; Martini, S. The Utilization of Algae and Seaweed Biomass for Bioremediation of Heavy Metal-Contaminated Wastewater. *Molecules* **2022**, *27*, 1275. [[CrossRef](#)]
19. Guleria, A.; Kumari, G.; Lima, E.C.; Ashish, D.K.; Thakur, V.; Singh, K. Removal of inorganic toxic contaminants from wastewater using sustainable biomass: A review. *Sci. Total Environ.* **2022**, *823*, 153689. [[CrossRef](#)]
20. Suhas; Gupta, V.K.; Carrott, P.J.M.; Singh, R.; Chaudhary, M.; Kushwaha, S. Cellulose: A review as natural, modified and activated carbon adsorbent. *Bioresour. Technol.* **2016**, *216*, 1066–1076. [[CrossRef](#)]
21. Suhas; Carrott, P.J.M.; Ribeiro Carrott, M.M.L. Lignin—From natural adsorbent to activated carbon: A review. *Bioresour. Technol.* **2007**, *98*, 2301–2312. [[CrossRef](#)] [[PubMed](#)]
22. Deshmukh, P.; Sar, S.K.; Ghosh, P.K. Efficient exclusion of uranyl ion from aqueous medium by a novel magnetic bio adsorbent (*Phyllanthus emblica* bark). *Groundw. Sustain. Dev.* **2021**, *14*, 100625. [[CrossRef](#)]
23. Verma, R.; Kundu, L.M.; Pandey, L.M. Enhanced melanoidin removal by amine-modified *Phyllanthus emblica* leaf powder. *Bioresour. Technol.* **2021**, *339*, 125572. [[CrossRef](#)] [[PubMed](#)]
24. Gaire, B.P.; Subedi, L. Phytochemistry, pharmacology and medicinal properties of *Phyllanthus emblica* Linn. *Chin. J. Integr. Med.* **2014**. *Online ahead of print.* [[CrossRef](#)]
25. Ahmad, B.; Hafeez, N.; Rauf, A.; Bashir, S.; Linfang, H.; Rehman, M.-u.; Mubarak, M.S.; Uddin, M.S.; Bawazeer, S.; Shariati, M.A.; et al. *Phyllanthus emblica*: A comprehensive review of its therapeutic benefits. *S. Afr. J. Bot.* **2021**, *138*, 278–310. [[CrossRef](#)]
26. Poltanov, E.A.; Shikov, A.N.; Dorman, H.J.D.; Pozharitskaya, O.N.; Makarov, V.G.; Tikhonov, V.P.; Hiltunen, R. Chemical and antioxidant evaluation of Indian gooseberry (*emblica officinalis* Gaertn., syn. *Phyllanthus emblica* L.) supplements. *Phytother. Res.* **2009**, *23*, 1309–1315. [[CrossRef](#)]
27. Pehlivan, E.; Altun, T.; Cetin, S.; Iqbal Bhangar, M. Lead sorption by waste biomass of hazelnut and almond shell. *J. Hazard. Mater.* **2009**, *167*, 1203–1208. [[CrossRef](#)]
28. Javanbakht, V.; Zilouei, H.; Karimi, K. Lead biosorption by different morphologies of fungus *Mucor indicus*. *Int. Biodeterior. Biodegrad.* **2011**, *65*, 294–300. [[CrossRef](#)]

29. Hossain, A.; Bhattacharyya, S.R.; Aditya, G. Biosorption of cadmium by waste shell dust of fresh water mussel *Lamellidens marginalis*: Implications for metal bioremediation. *ACS Sustain. Chem. Eng.* **2014**, *3*, 1–8. [[CrossRef](#)]
30. Nadeem, M.; Mahmood, A.; Shahid, S.A.; Shah, S.S.; Khalid, A.M.; McKay, G. Sorption of lead from aqueous solution by chemically modified carbon adsorbents. *J. Hazard. Mater.* **2006**, *138*, 604–613. [[CrossRef](#)]
31. Zhang, M.; Yin, Q.; Ji, X.; Wang, F.; Gao, X.; Zhao, M. High and fast adsorption of Cd(II) and Pb(II) ions from aqueous solutions by a waste biomass based hydrogel. *Sci. Rep.* **2020**, *10*, 3285. [[CrossRef](#)] [[PubMed](#)]
32. Yuvaraja, G.; Krishnaiah, N.; Subbaiah, M.V.; Krishnaiah, A. Biosorption of Pb(II) from aqueous solution by *Solanum melongena* leaf powder as a low-cost biosorbent prepared from agricultural waste. *Colloids Surf. B Biointerfaces* **2014**, *114*, 75–81. [[CrossRef](#)] [[PubMed](#)]
33. Langmuir, I. The adsorption of gases on plane surfaces of glass, mica and platinum. *J. Am. Chem. Soc.* **1918**, *40*, 1361–1403. [[CrossRef](#)]
34. Freundlich, H.M.F. Over the adsorption in solution. *J. Phys. Chem.* **1906**, *57*, 385–470.
35. Fifi, U.; Winiarski, T.; Emmanuel, E. Assessing the mobility of lead, copper and cadmium in a calcareous soil of Port-au-Prince, Haiti. *Int. J. Environ. Res. Public Health* **2013**, *10*, 5830–5843. [[CrossRef](#)]
36. Weber, T.W.; Chakravorti, R.K. Pore and solid diffusion models for fixed-bed adsorbers. *AIChE J.* **1974**, *20*, 228–238. [[CrossRef](#)]
37. Suhas; Gupta, V.K.; Singh, L.P.; Chaudhary, M.; Kushwaha, S. A novel approach to develop activated carbon by an ingenious hydrothermal treatment methodology using *Phyllanthus emblica* fruit stone. *J. Clean. Prod.* **2021**, *288*, 125643. [[CrossRef](#)]
38. Rambabu, K.; Thanigaivelan, A.; Bharath, G.; Sivarajasekar, N.; Banat, F.; Show, P.L. Biosorption potential of *Phoenix dactylifera* coir wastes for toxic hexavalent chromium sequestration. *Chemosphere* **2021**, *268*, 128809. [[CrossRef](#)]
39. Cholicó-González, D.; Ortiz Lara, N.; Fernández Macedo, A.M.; Chavez Salas, J. Adsorption Behavior of Pb(II), Cd(II), and Zn(II) onto Agave Bagasse, Characterization, and Mechanism. *ACS Omega* **2020**, *5*, 3302–3314. [[CrossRef](#)]
40. Fabre, E.; Lopes, C.B.; Vale, C.; Pereira, E.; Silva, C.M. Valuation of banana peels as an effective biosorbent for mercury removal under low environmental concentrations. *Sci. Total Environ.* **2020**, *709*, 135883. [[CrossRef](#)]
41. Huang, D.; Li, B.; Ou, J.; Xue, W.; Li, J.; Li, Z.; Li, T.; Chen, S.; Deng, R.; Guo, X. Megamerger of biosorbents and catalytic technologies for the removal of heavy metals from wastewater: Preparation, final disposal, mechanism and influencing factors. *J. Environ. Manag.* **2020**, *261*, 109879. [[CrossRef](#)] [[PubMed](#)]
42. Wang, Q.; Wang, Y.; Yang, Z.; Han, W.; Yuan, L.; Zhang, L.; Huang, X. Efficient removal of Pb(II) and Cd(II) from aqueous solutions by mango seed biosorbent. *Chem. Eng. J. Adv.* **2022**, *11*, 100295. [[CrossRef](#)]
43. Chen, H.; Zhao, J.; Dai, G.; Wu, J.; Yan, H. Adsorption characteristics of Pb(II) from aqueous solution onto a natural biosorbent, fallen *Cinnamomum camphora* leaves. *Desalination* **2010**, *262*, 174–182. [[CrossRef](#)]
44. Mwandira, W.; Nakashima, K.; Kawasaki, S.; Arabelo, A.; Banda, K.; Nyambe, I.; Chirwa, M.; Ito, M.; Sato, T.; Igarashi, T.; et al. Biosorption of Pb(II) and Zn(II) from aqueous solution by *Oceanobacillus profundus* isolated from an abandoned mine. *Sci. Rep.* **2020**, *10*, 21189. [[CrossRef](#)]
45. Taşar, Ş.; Kaya, F.; Özer, A. Biosorption of lead(II) ions from aqueous solution by peanut shells: Equilibrium, thermodynamic and kinetic studies. *J. Environ. Chem. Eng.* **2014**, *2*, 1018–1026. [[CrossRef](#)]
46. Lagergren, S. About the theory of so-called adsorption of soluble substances. *Kungliga Sven. Vetensk. Handlingar.* **1898**, *24*, 1–39.
47. Ho, Y.S.; McKay, G. Pseudo-second order model for sorption processes. *Process Biochem.* **1999**, *34*, 451–465. [[CrossRef](#)]
48. Ho, Y.S.; Chiang, C.C. Sorption Studies of Acid Dye by Mixed Sorbents. *Adsorption* **2001**, *7*, 139–147. [[CrossRef](#)]
49. Ho, Y.S.; McKay, G. Sorption of dye from aqueous solution by peat. *Chem. Eng. J.* **1998**, *70*, 115–124. [[CrossRef](#)]